

# Probability distributions for kinetic roughening in the Kardar-Parisi-Zhang growth with long-range temporal and spatial correlations

Zhichao Chang and Hui Xia\*

*School of Materials Science and Physics, China University of Mining and Technology, Xuzhou 221116, China*

(Dated: May 18, 2022)

We investigate numerically the effects of long-range temporal and spatial correlations based on probability distribution of interface width  $W(L, t)$  in the (1+1)-dimensional Kardar-Parisi-Zhang (KPZ) growth system. Through extensive numerical simulations, we find that long-range temporally correlated noise could impact the distribution form of interface width. Generally,  $W(L, t)$  obeys lognormal distribution when the temporal correlation exponent  $\theta$  is beyond a critical threshold, in comparison with Tracy-Widom Gaussian symplectic ensembles (TW-GSE) with Gaussian noise. On the other hand, the effects of long-range spatially correlated noise on the KPZ system are very different. Our results show that the distribution form of  $W(L, t)$  continuously varies with changing the spatial correlation exponent  $\rho$ . As  $\rho$  increases, the distribution becomes more asymmetric, leptokurtic, and fat-tailed, and tends to an unknown form, in a certain sense, which is similar to generalized extreme value (GEV) distribution.

## I. INTRODUCTION

Nonequilibrium processes are common in nature, which play indispensable roles in many actual physical phenomena, such as kinetic roughening, turbulence, combustion and active matter, among others [1–3]. As a typical nonequilibrium system, kinetic roughening has received much attention for several decades[1, 4–7]. The Kardar-Parisi-Zhang (KPZ) equation, which was originally used to describe kinetic roughening process[4], is one of the most important nonlinear Langevin-type growth equations in this field, and it can also be observed in many other fields[1, 2, 8–12]. The KPZ equation in the (1+1)-dimensions reads[4],

$$\frac{\partial h(x, t)}{\partial t} = \nu \nabla^2 h + \frac{\lambda}{2} (\nabla h)^2 + \eta(x, t), \quad (1)$$

where  $h(x, t)$  is the interface height in position  $x$  and time  $t$ ,  $\nu$  is the surface tension describing relaxation of the interface,  $\lambda$  is the nonlinear coefficient, representing lateral growth, and  $\eta(x, t)$  is stochastic force that usually is uncorrelated

$$\langle \eta(x, t) \eta(x', t') \rangle \sim \delta(x - x') \delta(t - t'). \quad (2)$$

Previous research has indicated that surface roughening processes exhibit scaling behaviors[5, 13–15], which are often characterized by the rms fluctuation of surface and interface height. To describe the characteristic of kinetic roughening, one often uses interface width that is defined by[1]

$$W(L, t) = \left\langle \sqrt{\frac{1}{L} \sum_x [h(x, t) - \bar{h}(t)]^2} \right\rangle^{1/2}, \quad (3)$$

where  $\bar{h}(t)$  is the mean height of rough interface with substrate size  $L$ ,  $\langle \dots \rangle$  stands for the average over different noise. And  $W(L, t)$  follows a dynamic scaling form[5]:

$$W(L, t) \sim \begin{cases} t^\beta, & \text{for } t \ll t_\times, \\ L^\alpha, & \text{for } t \gg t_\times, \end{cases} \quad (4)$$

where  $\beta$  is growth exponent,  $\alpha$  is roughness exponent, and  $t_\times \sim L^z$  with dynamic exponent  $z = \alpha/\beta$ . These scaling exponents could reveal plenty of dynamic scaling properties of surface and interface growth[1].

The (1+1)-dimensional KPZ equation with Gaussian noise has well studied in recent decades, scaling exponents and universal distributions are also obtained exactly[16–18]. However, the KPZ equation driven by long-range temporally or spatially correlated noise is more complicated and the exact solutions are still lacking. Fortunately, based on numerical simulations and analytic approximate techniques, for example, dynamic renormalization group (DRG)[19] and self-consistent expansion (SCE)[20, 21], a lot of rich analytical predictions and numerical results have been achieved. But, generally speaking, the discrepancy among these theoretical predictions and numerical solutions is still very obvious[19–22].

Previous research mainly focused on the KPZ equation with long-range spatial correlations rather than those with long-range temporal correlations [6, 20, 23–39]. Although recent studies about temporal correlated KPZ equation filled partial research gaps[21, 22, 40–44], some contradictory issues need further clarification. It is generally agreed that long-rang correlations could affect scaling properties of KPZ growth[1, 7], while some disagreements still exist from the perspective of the estimated values of critical exponents. This motivates us to investigate the effects of long-range temporal and spatial correlations on the continuous KPZ system with the help of the probability distribution, which allows one to obtain more fundamental and essential characteristics. In our work, we firstly examine scaling exponents of the KPZ system driven by long-range correlated noises, and then investigate if and how long-range temporal and spatial correlations impact the probability distributions of  $W(L, t)$ , and what are characteristics and differences of

\* Corresponding author: hxia@cumt.edu.cn

probability distributions in the KPZ growth driven by these two long-range correlated noises.

The paper is organized as follows: Firstly, we introduce the method to generate long-range correlated noises. And then, we describe one of the improved versions of the finite-difference (FD) method for direct simulating the KPZ equation driven by long-range temporally and spatially correlated noises. Next, we exhibit our numerical simulations and compare them with previous research. Finally, the corresponding discussions and conclusions are given.

## II. BASIC METHODS AND CONCEPTS

### II.1. Generating long-range correlated noises

When the noise have long-range temporal and spatial correlations, these two  $\delta$  functions of Eq. (2) are replaced by the term that decays as a power of time and distance. Thus, the second moment of the correlated noise is given by

$$\langle \eta(x, t) \eta(x', t') \rangle \sim |x - x'|^{2\rho-1} |t - t'|^{2\theta-1}, \quad (5)$$

where  $\rho$  and  $\theta$  are the spatial and temporal correlation exponents, respectively. If  $\rho = 0$  and  $\theta \neq 0$ , the noise is long-range temporally correlated case, on the contrary, the noise has long-range correlations in space.

To generate long series of correlated noise, we adopt the fast fractional Gaussian noise (FFGN) method, which was first proposed by Mandelbrot[45]. One starts by generating a series of uncorrelated uniformly distribution numbers  $\xi(u)$  in the range  $[0, 1]$ . The weight function is given by

$$W_n^2 = \frac{12(1 - r_n^2) \left( B^{\frac{1}{2}-\varphi} - B^{\varphi-\frac{1}{2}} \right) (aB^{-n})^{1-2\varphi}}{\Gamma(2-2\varphi)}, \quad (6)$$

where  $r_n = e^{-u_n}$  with  $u_n = aB^{-n}$ ,  $B = 2$ , and  $a = 6$ .  $\Gamma(\dots)$  is Gamma function, and  $\varphi$  represents temporal or spatial correlation exponent. And then, two autocorrelation decaying functions are defined by

$$\begin{aligned} X_1(u) &= [\xi_1(u) - 0.5] / \sqrt{1 - r^2}, \quad \text{for } t = 1, \\ X_n(u) &= rX_{t-1}(u) + [\xi_t(u) - 0.5], \quad \text{for } t > 1. \end{aligned} \quad (7)$$

---


$$\Psi(x, t) = \frac{1}{3} \left\{ [h(x+1, t) - h(x, t)]^2 + [h(x+1, t) - h(x, t)][h(x, t) - h(x-1, t)] + [h(x, t) - h(x-1, t)]^2 \right\} / \Delta x^2. \quad (11)$$


---

In our following simulations, the time evolution of interface starts from an initially flat  $h(x, 0) = 0$  with periodic boundary conditions. We set  $\nu = 1$ ,  $\Delta t = 0.05$ ,  $\Delta x = 1$ , and  $\eta(x, t)$  is long-range temporally or spatially correlated noise generated by FFGN. And then, we need to adjust  $\lambda$  for a given temporal or spatial correlated

Finally, one can obtain the long-range correlated noise

$$\eta = \sum_{n=1}^N W_n X_t(u_n), \quad (8)$$

where  $N$  is the number of components needed, which should be increased to obtain the desired power-law exponent  $\varphi$  with higher precision at low frequencies.

### II.2. The discretized schemes of (1+1)-dimensional KPZ equation

FD method is one of the most direct and common numerical tools. Theoretically, the differential interval is enough small, and the numerical results one obtained will be more accurate. Unfortunately, numerical divergence in simulating the nonlinear KPZ system could not be avoided based on the standard FD method. In order to suppress the annoying growth instability, an exponentially decaying function was suggested to replace the nonlinear term, which could be partially effective at suppressing numerical instability[46]. However, this exponentially decaying technique including infinitely many higher-order nonlinearities may cause nontrivial scaling behavior[47, 48]. Interestingly, an improved FD method proposed by Lam and Shin (LS)[49] could suppress effectively numerical divergence in comparison with the normal FD scheme. Thus, the discretized KPZ equation with LS scheme in the (1+1)-dimensions has the following form,

$$h(x, t+1) = h(x, t) + \Delta t \left[ \nu \Phi(x, t) + \frac{\lambda}{2} \Psi(x, t) + \eta(x, t) \right]. \quad (9)$$

Here, the discretized diffusive term  $\Phi(x, t)$  reads

$$\Phi(x, t) = [h(x+1, t) - 2h(x, t) + h(x-1, t)] / \Delta x^2, \quad (10)$$

and the nonlinear term  $\Psi(x, t)$  is discretized as

---

exponent in order to ensure into the true KPZ scaling regime before numerical divergence appearing.

### II.3. Skewness and kurtosis of statistical distribution

For a series of random variables  $X_i$  that obey a certain distribution, skewness ( $S$ ) could describe asymmetry of the distribution and is defined by

$$S = \frac{1}{n} \sum_{i=1}^n \left[ \left( \frac{X_i - \mu}{\sigma} \right)^3 \right], \quad (12)$$

where  $\mu$  is the mean value and  $\sigma$  is the standard deviation.  $S = 0$  means the distribution is symmetric,  $S < 0$  is called as the positive skewness representing the distribution incline to left, on the contrary,  $S > 0$  is negative skewness, and the distribution inclines to right.

Kurtosis ( $K$ ) is another important statistic, which could describe the steepness of distribution,

$$K = \frac{1}{n} \sum_{i=1}^n \left[ \left( \frac{X_i - \mu}{\sigma} \right)^4 \right]. \quad (13)$$

$K = 3$  represents the normal distribution,  $K < 3$  means the distribution is more smooth than the normal distribution, and  $K > 3$  indicates the distribution exhibits more steep than the normal one. According to measuring  $S$  and  $K$ , one could compare a given distribution from a normal case and then estimate its specific form.

## III. NUMERICAL RESULTS AND DISCUSSIONS

### III.1. The KPZ equation with long-range temporal correlations

In this subsection, we investigate numerically the temporal correlated KPZ system in the (1+1)-dimensions based on LS numerical scheme. To study the effects of long-range temporal correlations on probability distribution for kinetic roughening within the early growth regimes, we calculate the time evolution of growth height and  $W(L, t)$ . Here, system size  $L = 4096$  and growth time  $t = 300$  are used. The distributions for  $W(L, t)$  with different  $\theta$  in the range  $[0, 0.40]$  are shown in Fig.1. Our results indicate that, when  $\theta > 0$ , every distribution is positive skewness, meanwhile, it has a longer tail in the right part, which fits highly the lognormal distribution. In the particular case, the distribution for  $\theta = 0$  (white noise) obeys Tracy-Widom Gaussian symplectic ensembles (TW-GSE)[50].

Considering that both  $S$  and  $K$  of the lognormal distribution are not constant, we need to analyze the logarithm of  $W(L, t)$  to check whether or not it obeys the normal distribution. Figure 2 shows  $S$  and  $K$  of  $\ln W$  for different  $\theta$ . We find that both  $S$  and  $K$  are generally consistent with the corresponding values of Gaussian distribution. However, we also notice that, with  $\theta$  increasing,  $S$  exists a little increasing trend. To explore the slight change, we adopt a quantile-quantile plot (Q-Q plot), a method

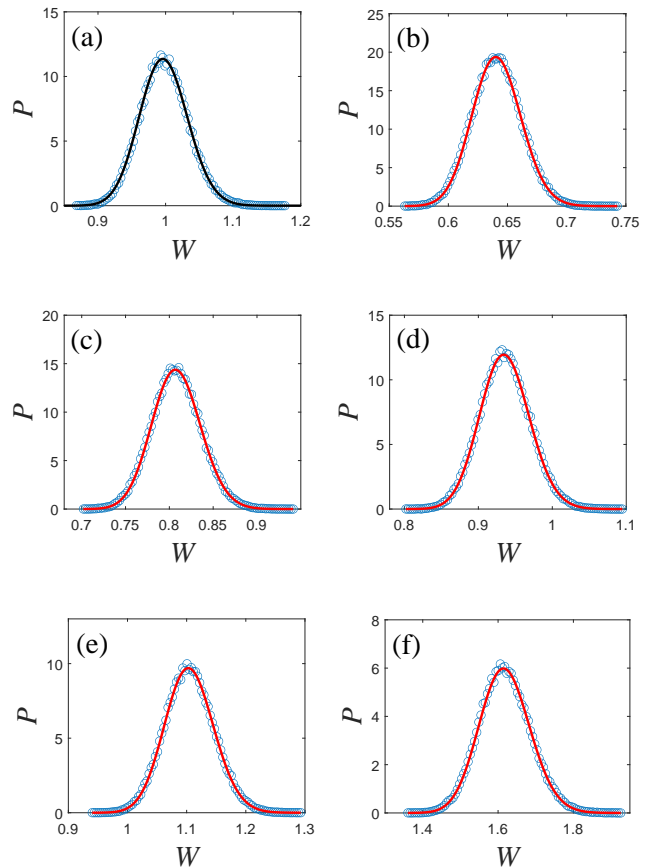


FIG. 1: Probability distributions for  $W(L, t)$  in the temporal correlated KPZ equation with different  $\theta$ : (a)  $\theta = 0.00$ , (b)  $\theta = 0.10$ , (c)  $\theta = 0.20$ , (d)  $\theta = 0.25$ , (e)  $\theta = 0.30$ , (f)  $\theta = 0.40$ . All data are averaged over  $10^5$  independent realizations. Comparisons with (a) TW-GSE (black solid line) and (b-f) lognormal distribution (red solid line) are also provided correspondingly.

to determine intuitively whether two series of numbers obey the same distribution, to analyze simulation data mentioned above. The corresponding results of the Q-Q plot are shown in Fig.3. Through quantitative comparison of TW-GSE ( $Q_{TW-GSE}$ ) and lognormal distribution ( $Q_{lognormal}$ ) with simulation data ( $Q_{Data}$ ), we find that distributions of  $W(L, t)$  are obey lognormal distribution when  $\theta > 0$ . Thus, these results show that long-range temporally correlated noise could change the distribution form of  $W(L, t)$  for the KPZ growth from normal to lognormal distribution, which also implies the slow variations of  $S$  and  $K$  are likely to measure errors due to extreme values.

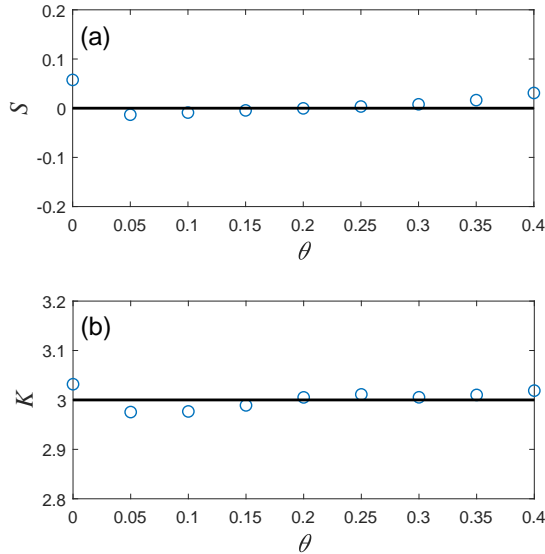


FIG. 2: The estimated values of (a) Skewness  $S$  and (b) kurtosis  $K$  for probability distributions of  $\ln W$  for KPZ model with long-range temporal correlations. The Gaussian distribution values (solid lines) are provided for quantitative comparison.

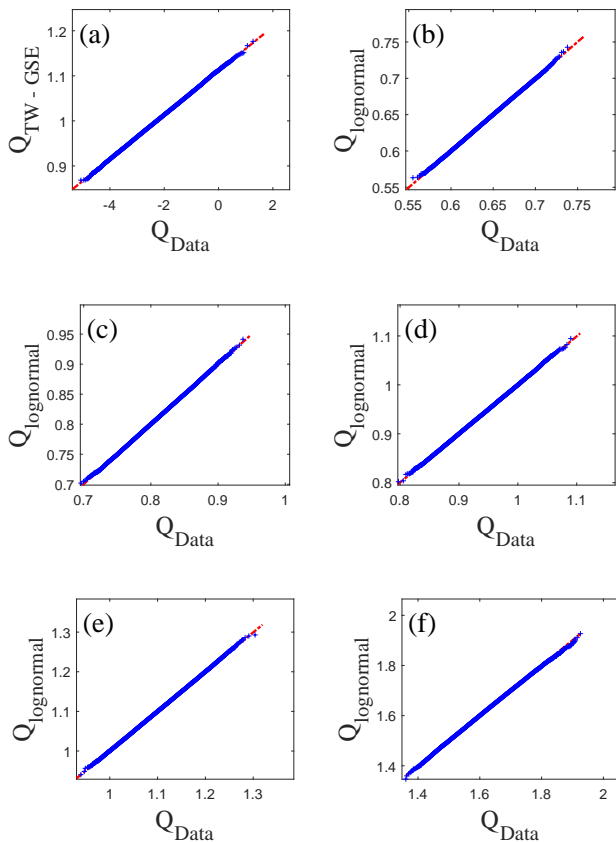


FIG. 3: The Q-Q plots of TW-GSE or lognormal distribution versus simulation data for different  $\theta$ . The values of  $\theta$  chosen here are same with Fig.1.

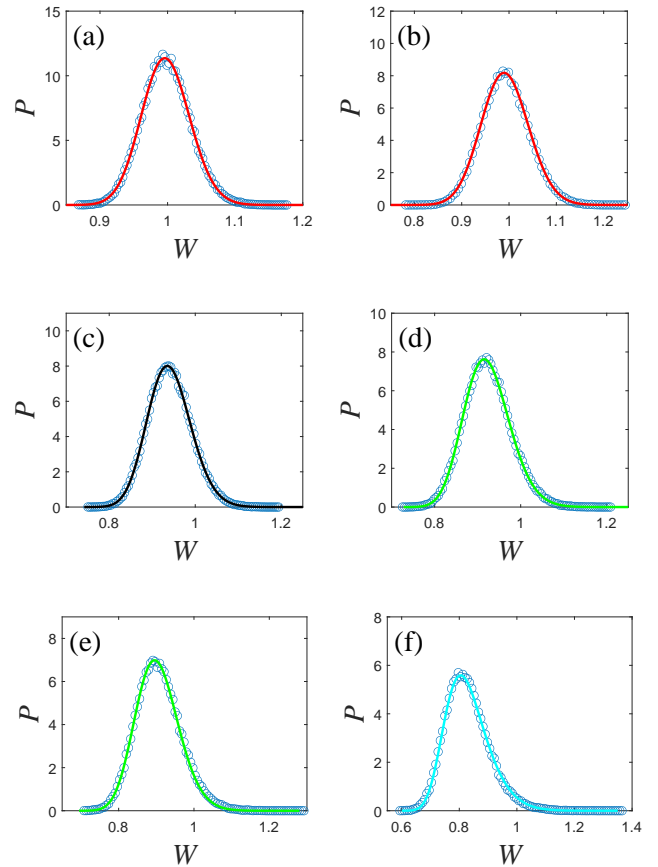


FIG. 4: Probability distributions for  $W(L, t)$  in the spatial correlated KPZ system with different  $\rho$ : (a)  $\rho = 0.00$ , (b)  $\rho = 0.10$ , (c)  $\rho = 0.20$ , (d)  $\rho = 0.25$ , (e)  $\rho = 0.30$ , (f)  $\rho = 0.40$ . All data are averaged over  $10^5$  independent realizations. The suitable distributions are provided for comparison: (a-b) TW-GSE (red solid line), (c) TW-GUE (black solid line), (d-e) TW-GOE (green solid line), and (f) GEV distribution (blue solid line).

### III.2. The KPZ equation with long-range spatial correlations

To investigate probability distributions for interface width of the spatial correlated KPZ system in the early growth regime, we perform numerical simulations with different spatial correlation exponent  $\rho$ . System size  $L = 4096$  and growth time  $t = 300$  are used, and numerical results are presented in Fig.4. We find that the distributions of  $W(L, t)$  quantitatively fit TW-GSE when  $\rho \leq 0.15$ , and with  $\rho$  increasing, transfer continuously to the generalized extreme value (GEV) distribution. In particular, the distribution is similar to the Tracy-Widom Gaussian unitary ensembles (TW-GUE) for  $0.15 < \rho \leq 0.20$ , and the Tracy-Widom Gaussian orthogonal ensemble (TW-GOE) for  $0.20 < \rho \leq 0.30$ .

Furthermore, we also analyze the variations of  $S$  and  $K$  with different  $\rho$ , the corresponding results are shown

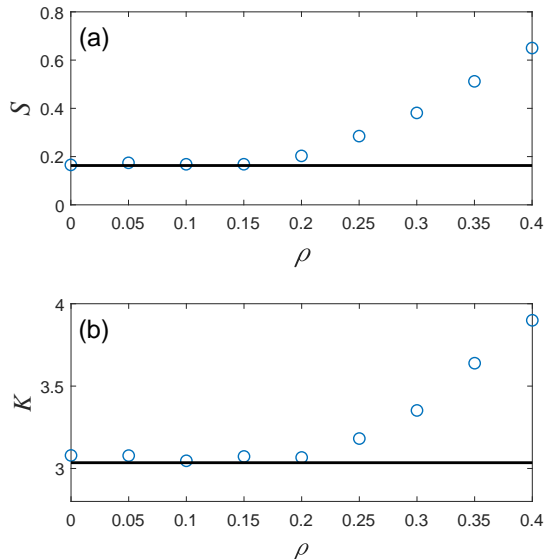


FIG. 5: The estimated values of (a) Skewness  $S$  and (b) kurtosis  $K$  for probability distributions for  $W(L, t)$  with different  $\rho$ , which compare quantitatively with the TW-GSE values (solid lines).

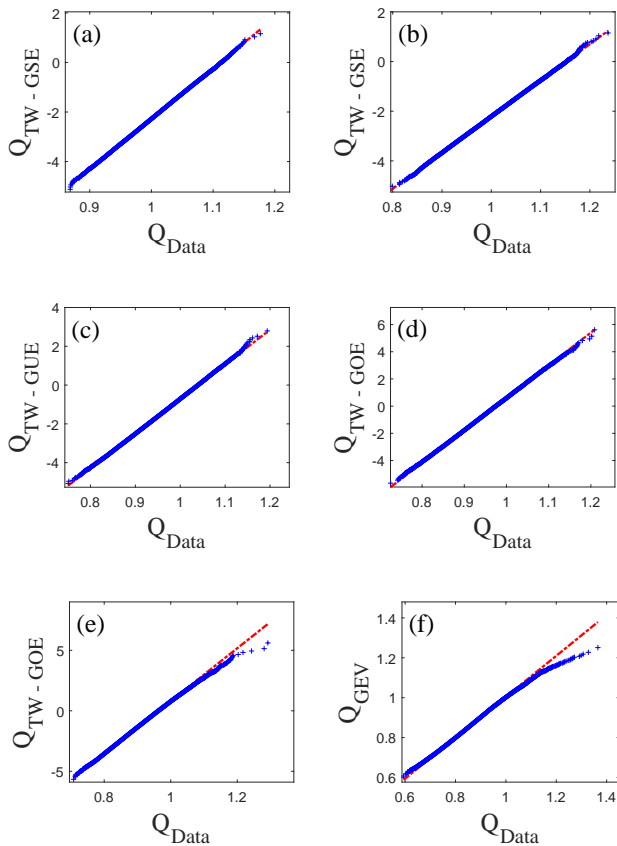


FIG. 6: The Q-Q plots of TW-GSE, TW-GUE, TW-GOE, GEV distribution versus simulation data for different  $\rho$ . The values of  $\rho$  chosen here are same with Fig.4.

in Figs.5(a) and 5(b), respectively. We find that, as  $\rho$  increases,  $S$  and  $K$  have similar changing trends. More specifically, both  $S$  and  $K$  approach the values of TW-GSE for  $\rho \leq 0.15$ , which indicates that the distribution form is not significantly affected by long-range spatially correlated noise within this correlated regime. When  $\rho > 0.15$ ,  $S$  and  $K$  appear to increase with  $\rho$ , the distribution becomes more right-skewed, and the distribution has more fat tail. These characteristics are also consistent with our numerical results, as shown in Fig.4. Finally, the distributions of  $W(L, t)$  are quantitatively similar to the distribution form of GEV.

Given the sensitivity to extreme values for  $S$  and  $K$ , these results obtained above have a little uncertainty, thus we turn to analyze data using the Q-Q plot method. However, the Q-Q plots for different  $\rho$  show different results from the predictions mentioned above, as shown in Fig.6. According to a comparison of the quantile of fitting distribution and simulation data, there exists an evident discrepancy in the Q-Q plot for  $\rho > 0.30$ , which implies that simulation data are not in agreement with the expected distributions, but are just similar to the point of view of measurement. As  $\rho$  increases, the distribution becomes more asymmetric, leptokurtic, and fat-tailed, and tends to an unknown distribution, in a certain sense, which is similar to the GEV distribution. Thus, it is not clear that which distribution of  $W(L, t)$  obeys when  $\rho > 0.30$ .

#### IV. CONCLUSIONS

In summary, we have performed extensive numerical investigations in a (1+1)-dimensional KPZ system with long-range temporally and spatially correlated noises. Our results show that long-range temporal and spatial correlations could significantly affect probability distributions of  $W(L, t)$ , and the nontrivial effects of long-range temporal and spatial correlations are obviously different. For KPZ driven by temporally correlated noise, probability distributions of  $W(L, t)$  for the temporal correlated KPZ equation are in quantitative agreement with lognormal distribution when  $\theta > 0$ , as a special case,  $W(L, t)$  obeys TW-GSE when  $\theta = 0$ . Interestingly, Q-Q plots further confirm the conclusion, although the variations of  $S$  and  $K$  do not show evident dependence on  $\theta$ . For the spatial correlated KPZ system, we find that distribution forms of  $W(L, t)$  are not affected by long-range spatially correlated noise for  $\rho \leq 0.15$ , which still belongs to TW-GSE based on several independent estimation methods. While for  $\rho \geq 0.15$ , distribution form significantly depends on  $\rho$ . And variations of  $S$  and  $K$  with  $\rho$  also show a strong and positive dependence on  $\rho$  for this correlated regime. Moreover, the distributions become more skew and thin as  $\rho$  increases. Finally, the distribution of  $W(L, t)$  is quantitatively similar to that of GEV, which implies that the spatial correlate KPZ equation smoothly tends to another universality class with increasing  $\rho$ . However, it is still unclear what type of

distribution for the spatial correlated KPZ system when

$\rho$  is beyond a certain critical threshold.

- 
- [1] A.-L. Barabási and H. E. Stanley, *Fractal concepts in surface growth* (Cambridge University Press, Cambridge, UK, 1995).
- [2] L. Chen, C. F. Lee, and J. Toner, Nat. Commun. **7**, 12215 (2016).
- [3] D. Veynante and L. Vervisch, Prog. Energy Combust. Sci. **28**, 193 (2002).
- [4] M. Kardar, G. Parisi, and Y.-C. Zhang, Phys. Rev. Lett **56**, 889 (1986).
- [5] F. Family and T. Vicsek, J. Phys. A: Math. Gen. **18**, L75 (1985).
- [6] S. Chu and M. Kardar, Phys. Rev. E **94**, 10101 (2016).
- [7] T. Halpin-Healy and Y.-C. Zhang, Physics Reports **254**, 215 (1995).
- [8] D. Squizzato, L. Canet, and A. Minguzzi, Phys. Rev. B **97**, 195453 (2018).
- [9] M. Kulkarni and A. Lamacraft, Phys. Rev. A **88**, 021603 (2013).
- [10] V. N. Gladilin, K. Ji, and M. Wouters, Phys. Rev. A **90**, 023615 (2014).
- [11] E. Altman, L. M. Sieberer, and L. Chen, Phys. Rev. X **5**, 011017 (2015).
- [12] S. Mathey, T. Gasenzer, and J. M. Pawłowski, Phys. Rev. A **92**, 023635 (2015).
- [13] Y.-C. Zhang, Phys. Rev. B **42**, 4897 (1990).
- [14] H. G. Hentschel and F. Family, Phys. Rev. Lett **66**, 1982 (1991).
- [15] Hanfei and B.-K. Ma, Phys. Rev. E **47**, 3738 (1993).
- [16] M. Prähofer and H. Spohn, Phys. Rev. Lett **84**, 488488 (2000).
- [17] T. Sasamoto and H. Spohn, Phys. Rev. Lett **104**, 230602 (2010).
- [18] T. Halpin-Healy, Phys. Rev. Lett **109**, 170602 (2012).
- [19] E. Medina, T. Haw, M. Kardar, and Y.-C. Zhang, Phys. Rev. A **39**, 3053 (1989).
- [20] E. Katzav and M. Schwartz, Phys. Rev. E **60**, 5677 (1999).
- [21] E. Katzav and M. Schwartz, Phys. Rev. E **70**, 011601 (2004).
- [22] T. Song and H. Xia, Phys. Rev. E **103**, 012121 (2021).
- [23] P. Meakin and R. Jullien, Europhys. Lett. **9**, 71 (1989).
- [24] P. Meakin and R. Jullien, Phys. Rev. A **41**, 983 (1990).
- [25] J. G. Amar, P.-M. Lam, and F. Family, Phys. Rev. A **43**, 4548 (1991).
- [26] C. K. Peng, S. Havlin, M. Schwartz, and H. E. Stanley, Phys. Rev. A **44**, R2239 (1991).
- [27] N. N. Pang, Y. K. Yu, and T. Halpin-Healy, Phys. Rev. E **52**, 3224 (1995).
- [28] S. Mukherji and S. M. Bhattacharjee, Phys. Rev. Lett **79**, 2502 (1997).
- [29] M. S. Li, Phys. Rev. E **55**, 1178 (1997).
- [30] A. K. Chattopadhyay and J. K. Bhattacharjee, Europhys. Lett. **42**, 119 (1998).
- [31] E. Frey, U. C. Täuber, and H. K. Janssen, Europhys. Lett. **47**, 14 (1999).
- [32] M. K. Verma, Physica A: Statistical Mechanics and its Applications **392**, 100 (2006).
- [33] E. Katzav, Phys. Rev. E **68**, 046113 (2003).
- [34] E. Katzav, Eur. Phys. J. B **54**, 137 (2006).
- [35] E. Katzav, Physica A: Statistical Mechanics and its Applications **392**, 100 (2006).
- [36] T. Kloss, L. Canet, B. Delamotte, and N. Wschebor, Phys. Rev. E **89**, 022108 (2014).
- [37] P. A. Morais, E. A. Oliveira, N. A. M. Araújo, H. J. Herrmann, and J. S. A. Jr., Phys. Rev. E **84**, 016102 (2011).
- [38] H. Xia, T. Gang, and Y. Lan, Phys. Rev. E **94**, 062121 (2016).
- [39] O. Niggemann and H. Hinrichsen, Phys. Rev. E **97**, 062125 (2018).
- [40] C.-H. Lam, L. M. Sander, and D. F. Wolf, Phys. Rev. A **46**, R6128 (1992).
- [41] P. Strack, Phys. Rev. E **91**, 032131 (2015).
- [42] T. Song and H. Xia, J. Stat. Mech. **2016**, 113206 (2016).
- [43] D. Squizzato and L. Canet, Phys. Rev. E **100**, 062143 (2019).
- [44] A. Alés and J. M. López, Phys. Rev. E **99**, 062139 (2019).
- [45] B. B. Mandelbrot, Water Resources Research **7**, 543 (1971).
- [46] C. Dasgupta, J. M. Kim, M. Dutta, and S. D. Sarma, Phys. Rev. E **55**, 2235 (1997).
- [47] R. Gallego, M. Castro, and J. M. López, Eur. Phys. J. B. **89**, 189 (2016).
- [48] B. Li, Z. Tan, Y. Jiao, and H. Xia, J. Stat. Mech. **2021**, 023210 (2021).
- [49] C.-H. Lam and F. G. Shin, Phys. Rev. E **58**, 5592 (1998).
- [50] I. Corwin, Random Matrices: Theory Appl. **1**, 1130001 (2011).